

Gelation and Phase Equilibria of Responsive Elastin-Mimetic Triblock Hydrogels

D. S. Hart¹, A. J. M. D'Souza², C. R. Middaugh³, and S. H. Gehrke^{1,3}

¹Dept. of Chemical & Petroleum Engineering, The University of Kansas, Lawrence, KS 66045

²Department of Molecular Biology, University of Wyoming, Laramie, WY 82071

³Department of Pharmaceutical Chemistry, The University of Kansas, Lawrence, KS 66045

Introduction:

Elastin-mimetic triblock (EMT) polypeptides can thermally gel in aqueous solution upon heating to form a stable three-dimensional polymer network. This polypeptide is based on the amino acid sequence of elastin (VPGVG) and constructed as a BAB block copolymer. End B-blocks are relatively hydrophobic, while the center A-block is more hydrophilic. The network forms through the aggregation of the B blocks, and swells to equilibrium in excess water. Thermally-gelling polypeptides have significant potential for use in biomedical devices because they can form stable yet biodegradable networks at physiological conditions without the need for crosslinking agents. Furthermore, utilizing biomimetic polypeptide sequences which are present in human tissues could aid cellular recognition and response. A number of thermally gelling polypeptides based on biological motifs such as silk,¹ elastin,² or combinations thereof¹ have been created in recent years. Determination of the specific stabilizing interactions of thermal gelation is of importance to the *de novo* design of biomaterials for drug delivery or tissue engineering applications.

This work explores the development of these interactions during the sol-gel transition in elastin-mimetic triblock (EMT) polypeptides through two complementary vibrational spectroscopic techniques. Laser Raman spectroscopy and ATR-FTIR (attenuated total reflectance-Fourier transform infrared) spectroscopy were used to investigate the changes in secondary structure associated with this transition in H₂O and D₂O. The sol-gel transition is reversible, with gelation upon heating while the gel re-liquefies upon cooling. The sequence of this 135 kDa polypeptide is based upon the VPGVG pentamer repeat of elastin and has been constructed as a BAB block copolymer.³ The B-blocks are modified to be more hydrophobic than VPGVG with alanine (A) and isoleucine (I) incorporated into pentamers as VPAVG[(IPAVG)₄(VPAVG)]₁₆IPAVG, while the center A-block is modified to be more hydrophilic than elastin with some glutamic acid (E) substituted for V as VPGVG[(VPGVG)₂VPGE(VPGVG)₂]₃₀VPGVG. The network forms through aggregation of the B-blocks.³ This network organization has been shown to be interconnected through a uniformly dispersed set of micellar hydrophobic cores, through cryo-high resolution scanning electron microscopy.^{4,5}

Once these micellar interactions have formed to create the network, the gel swells to a stable equilibrium in excess water.^{3,6} As a hydrogel, the network is also thermally responsive: that is, it shrinks and swells in response to temperature changes. Therefore a phase diagram was developed to quantify the network's thermal responsiveness.⁶ Further investigation of this phase diagram has revealed a dependence of equilibrium swelling on synthesis conditions. This dependence suggests that the stabilizing interactions persist after network formation and do not reorganize above the gelation temperature.

Experimental:

Elastin-mimetic triblock polypeptides were expressed in *E. coli* and purified as described elsewhere.⁵ Lyophilized EMT was dissolved in either DIUF (deionized ultrafiltered) H₂O (Fisher Scientific) or D₂O (Sigma Aldrich) at 4°C for 2 hours to make 10% (w/w) solutions. The sol-gel transition occurred near 18°C in both H₂O and D₂O. Laser Raman spectra were

obtained from a Chromex Raman 2000 system with a 300 mW solid state diode laser at 785 nm equipped with Peltier temperature control. Each Raman spectrum was collected at a discrete temperature after the sample had attained thermal equilibrium for 20 min. Fourier-transform Infrared spectra were collected with an ABB Bomem PROTA with a ZnSe ATR crystal. The solution temperature was measured in the ATR cell as it warmed from 4°C to room temperature over a period of 30 minutes. ATR-FTIR Spectra were Fourier deconvoluted on GRAMS/AI software. Deconvoluted ATR-FTIR spectra and Raman spectra were peak fit with Gaussian and Lorentzian functions in the Amide I region (1600-1700 cm⁻¹).

In phase diagram investigations, hydrogels were synthesized as cylindrical discs in molds (radius = 0.3 cm, thickness = 0.16 cm) consisting of silicon rubber glued to Teflon[®]. 50-65 μL of DIUF water was injected into the mold, which was maintained at 4°C. Depending on the synthesis concentration desired, a given amount of lyophilized EMT (6-14 mg) was added to the mold well and allowed to dissolve. The liquid solution was gently stirred to homogeneity and then the mold (covered) was warmed to ambient temperature (~25°C), which induced the gelation of the solution. The discs were immersed into excess DIUF water at the appropriate temperature and allowed to equilibrate. Hydrogel masses typically reached constant values to ±1% within 24-48 h. The discs were then dried in a desiccator for 5 days to determine the mass of the polypeptide in the gel (80-90% polypeptide recovered). Differential scanning calorimetry (DSC) was employed to determine temperatures of gelation. These data were obtained with TA Instruments Q100 DSC and high volume stainless steel pans (100 μL). Approximately 70-95 μL of EMT in DIUF water at concentrations of 2.5, 5, 7.5, 10, and 12.5 wt% were each added to a high volume pan at 4°C with a positive displacement pipette (Gilson). The sample and reference cells were equilibrated at 4°C for approximately 10-15 minutes inside the DSC cell before each temperature scan. That thermal equilibrium was achieved was indicated by the heat flow attaining a constant value at nearly zero net heat flow (~ 1-2 mW/g). Three temperature scanning rates (1, 5, and 10°C/min) were used to estimate the true transition temperatures based on thermal lag in each concentration. The effect of thermal lag in DSC is well known, and its dependence can be removed through extrapolation to a zero scanning rate.^{7, 8}

Results:

Raman and ATR-FTIR were run as complementary probes of the events associated with the gelation of EMT. Raman spectra were collected on EMT solutions and the H₂O or D₂O background spectra were subtracted at each temperature. The spectra in D₂O are shown in Figure 1 a). In D₂O, five peaks were fit with average values of 1684, 1666, 1649, 1627, and 1609 cm⁻¹, whereas H₂O spectra gave peaks of 1684, 1667, 1646, 1628, and 1610 cm⁻¹. Raman peaks in the range of 1668-1677 cm⁻¹ have been shown to occur in peptides known to contain type I-III β-turns in D₂O.^{9, 10} Thomas *et al.* working with linear poly(VPGVG) (~100 kDa) obtained peaks which shifted near this frequency in H₂O, namely 1673 and 1650 cm⁻¹.¹¹ The peaks at 1646 and 1649 cm⁻¹ were assigned to a mixture of unordered structures and α-helices.¹² The peaks at 1627-1628 and 1684 cm⁻¹ are known to represent the low and high frequency shifts of β-sheet structures. Though the 1609 and 1610 cm⁻¹ peaks are typically assigned to tyrosine residues in Raman, EMT contains none. Thus it is more likely that these peaks can be identified with those of FTIR peaks in the 1610-1620 cm⁻¹ region, which have been attributed to extended hydrogen bonded structures, such as polyproline-II helices (PP-II) prior to aggregation.^{13, 14} The peaks at 1627 and 1628 cm⁻¹ increase with temperature, while the peaks at 1609 and 1610 cm⁻¹ substantially decrease (Figure 1 b) depicts the key peak area

trends associated with gelation). This increase in β -sheet structures during gelation is assumed to occur by aggregation of the B-blocks. In Figure 1 b) these extended hydrogen bonded structures minimally decrease during gelation while β -sheet increases. It is our hypothesis that it is this β -sheet formation that induces gelation of EMT in aqueous solution.

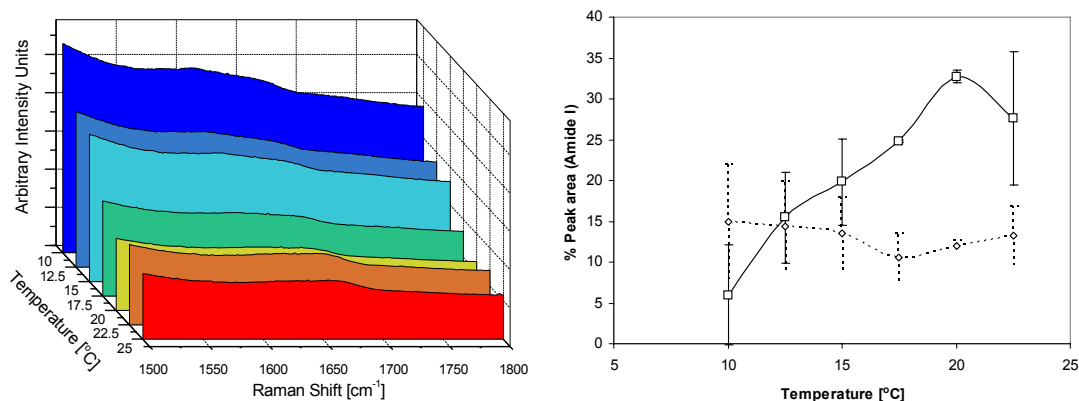


Figure 1. a) Amide I region of Raman spectra upon crossing the sol-gel transition ($\sim 17^\circ\text{C}$) of 10% (w/w) EMT in D_2O . **b)** Percent peak areas as obtained from peak fits with structure assignments indicated ($\text{---}\square\text{---}$) β -sheet (1627 cm^{-1}) and ($\text{---}\diamond\text{---}$) PP-II helices (1609 cm^{-1}).

For additional evidence of β -sheet formation during gelation, ATR-FTIR spectra were collected on EMT solutions of H_2O and D_2O . As shown in Figure 2 a), the most striking change during gelation is the apparent increase in the peak near 1620 cm^{-1} relative to 1640 cm^{-1} . To quantify this change, spectra were deconvoluted to yield three peaks centered at $1610\text{--}1625\text{ cm}^{-1}$, $1640\text{--}1655\text{ cm}^{-1}$ and $1660\text{--}1680\text{ cm}^{-1}$ (Figure 2 b). Peaks near 1620 cm^{-1} have traditionally been assigned as intermolecular β -sheets, which is hypothesized to occur from the intermolecular hydrophobic association of B-blocks.¹⁵ During gelation, peaks near 1610 cm^{-1} , which were assigned to PP-II type helices shifted to $1620\text{--}1625\text{ cm}^{-1}$, which were attributed to intermolecular β -sheets. This peak shift was significant for three separate trials (Figure 2 c) and implies that PP-II-like structures convert to intermolecular β -sheets during gelation. This peak shift is consistent with ATR-FTIR peak shifts of 5 wt% aqueous solutions of poly(AVGVP) and poly(GVGVP) (MW $\sim 100\text{ kDa}$).¹⁶ Peaks in the range of $1640\text{--}1648\text{ cm}^{-1}$ have been often attributed to unordered structures¹⁷ and peaks in the range of $1660\text{--}1680$ were attributed to Type II β -turns.¹⁸

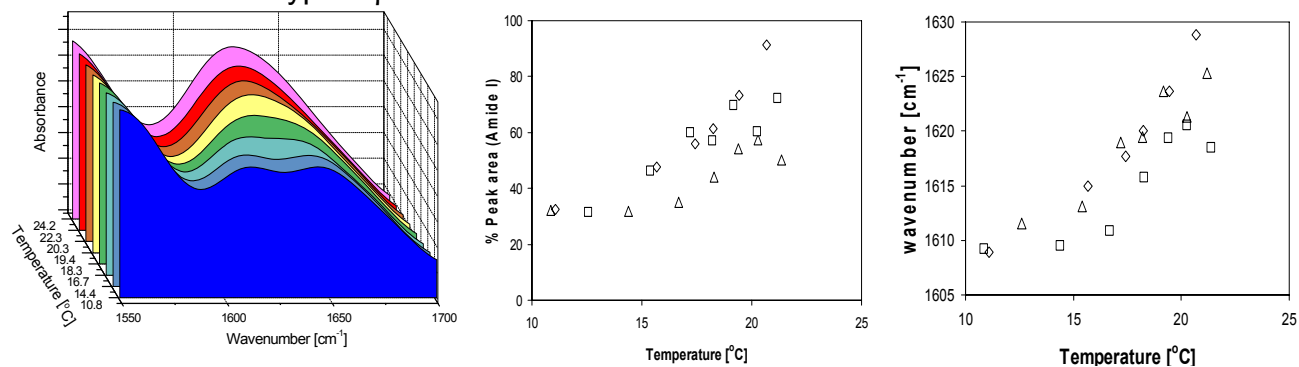


Figure 2. a) Amide I region of Raman spectra upon crossing the sol-gel transition of 10% (w/w) EMT in H_2O . **b)** Percent peak area of PP-II/ β -sheet as obtained from deconvolution and peak fits of three trials. **c)** Peak shift of PP-II to β -sheet. Each shape represents a different trial.

Once the stabilizing interactions have formed the network, EMT hydrogels placed in excess solvent swell to reach equilibrium with a sol phase. A temperature-composition phase diagram can be used to characterize both the swelling equilibria and phase boundaries of the sol and gel states. The lowest temperature at which phase separations occurs upon heating is known as the lower critical solution temperature (LCST). The LCST can be identified in physically gelling systems through the development of a phase diagram such as that shown in Figure 3 a. The tie line through the two phase region indicates the equilibrium of the hydrogel with its sol phase.

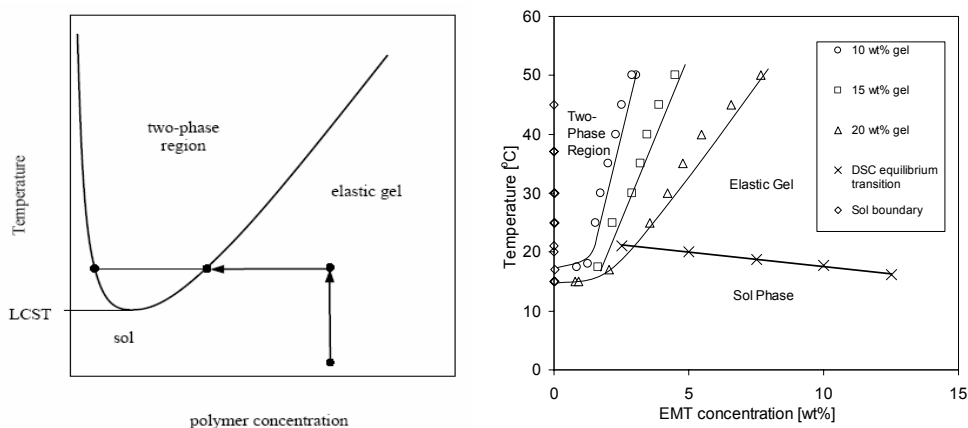


Figure 3. a) Generic temperature-composition phase diagram of a physical gel with LCST behavior (LCST $\sim 15^{\circ}\text{C}$). **b)** Temperature-composition phase diagram of EMT in water. The percentage indicates the EMT concentration at synthesis. Tie lines in two phase region are implied.

The swelling behavior of EMT in water is shown in Figure 3 b) with a temperature-composition phase diagram of gels formed at three different synthesis concentrations. This figure demonstrates the thermal-responsiveness of the gels above the gelation temperature, as the concentration in the gel phase increases with increasing temperature (i.e., they shrink). Very little polymer leaves the gel to enter the sol phase, which has a concentration of approximately 0.001 wt% (as determined by UV spectroscopy and mass balances) for all temperatures and concentrations examined in Figure 3 b). Further indication of the stability of the interactions which hold the network together is seen by the significantly different equilibrium swelling curves of the three different gel compositions. These results are in contrast to the phase equilibria of other micelle forming solutions like surfactants. Some of these micelle forming solutions also display LCST behavior in aqueous solution, such as meroxapols¹⁹ and noionic surfactants (e.g 3,6,9,12 tetraoxadocosanol).²⁰ Meroxapols are a family of triblock copolymers similar to the poloxamers sold under the tradename PluronicTM, except that the endblocks are hydrophobic (polypropylene oxide) and the centerblock is hydrophilic (polyethylene oxide), similar to EMT. Both types of these solutions form phase boundaries to the two phase-micellar region which are independent of starting synthesis concentration. This path-independence indicates that these micelles can reorganize to reach a true thermodynamic equilibrium. However, Figure 3 b) shows the path dependence for EMT swelling as shown by the dependence upon synthesis concentration on the phase equilibria of these hydrogels. Clearly, once the stabilizing interactions have formed in EMT hydrogels, the network junctions do not reorganize. However, since the hydrogels themselves are stable for

at least a month, it appears the stabilizing interactions themselves are thermodynamically stable.

Discussion:

Raman and ATR-FTIR show that β -sheet increases relative to unordered structures during gelation, though the change is more subtle than suggested by the macroscopic observation of gelation. In Raman, gelation is accompanied by an increase in β -sheet. An increase in β -sheet upon gelation is also shown in FTIR. It is hypothesized that the β -turn segments are localized to the A-block due to its high percentage of VPGVG pentamer repeats, while the B-block's intermolecular associations are β -sheets which increase with temperature.

In conclusion, the assignments from FTIR and Raman support the hypothesis that an increase in β -sheet act to stabilize the network during gelation. The stability of the network in excess solvent also suggest that, once formed these interactions persist. However, there is sufficient flexibility in the A-blocks to allow swelling and shrinking of the network post gelation. This behavior similar to that observed with covalently crosslinked responsive gels like poly(N-isopropylacrylamide) or crosslinked elastin, and thus it might find similar applications without the need for covalent crosslinking.

Acknowledgements:

This work was supported by KBRIN (Kansas Biomedical Research Infrastructure Network) Grant NIH 5P20 RR164575-02 and NIH NIGMS (National Institute of General Medical Sciences) Grant GM08359.

References:

1. Haider, M.; Megeed, Z.; Ghandehari, H. *Journal of Controlled Release* **2004**, 95, 1-26.
2. Chilkoti, A.; Dreher, M. R.; Meyer, D. E. *Advanced Drug Delivery Reviews* **2002**, 54, 1093-1111.
3. Wright, E. R.; Conticello, V. P. *Advanced Drug Delivery Reviews* **2002**, 54, 1057-1073.
4. Wright, E. R.; McMillan, R. A.; Cooper, A.; Apkarian, R. P.; Conticello, V. P. *Advanced Functional Materials* **2002**, 12, (2), 149-154.
5. Nagapudi, K.; Brinkman, W. T.; Leisen, J.; Thomas, B. S.; Wright, E. R.; Haller, C.; X. Wu; Apkarian, R. P.; Conticello, V. P.; Chaikof, E. L. *Macromolecules* **2005**, 28, 345-354.
6. Hart, D. S.; Hagan, S. H.; Conticello, V. P.; Gehrke, S. H. *Controlled Release Society Transactions* **2004**, 31, 133.
7. Illers, K. H. *European Polymer Journal* **1974**, 10, 911-916.
8. Bershtein, V. A.; Egorov, V. M., *Differential Scanning Calorimetry of Polymers: Physics, Chemistry, Analysis, Technology*. Ellis Horwood: New York, NY, 1994.
9. Ishizaki, H.; Balaram, P.; Nagaraj, R.; Venkatachalapathi, Y. V.; Tu, A. T. *Biophysical Journal* **1981**, 36, 509-517.
10. Seaton, B. A. *Spectrochimica Acta* **1986**, 42A, (2/3), 227-232.
11. Thomas, G. J.; Prescott, B.; Urry, D. W. *Biopolymers* **1987**, 26, 921-934.
12. Bandekar, J. *Biochimica et Biophysica Acta* **1992**, 1120, 123-143.
13. Muga, A.; Mantsch, H. H.; Surewicz, W. K. *Biochemistry* **1991**, 30, 7219-7224.
14. Lefèvre, T.; Subirade, M. *International Journal of Food Science and Technology* **1999**, 34, 419-428.
15. Clark, A. H.; Saunderson, D. H. P.; Suggett, A. *International Journal of Peptide and Protein Research* **1981**, 17, 352-364.
16. Schmidt, P.; Dybal, J.; Rodriguez-Cabello, J. C.; Reboto, V. *Biomacromolecules* **2005**, 6, 697-706.
17. Middaugh, C. R.; Mach, H.; Ryan, J. A.; Sanyal, G.; Volkin, D. B., *Infrared Spectroscopy*. In *Protein Stability and Folding*, Shirley, B. A., Ed. Humana Press: Totowa, New Jersey, 1995; Vol. 40, pp 137-156.
18. Vass, E.; Hollósi, M.; Besson, F.; Buchet, R. *Chemical Reviews* **2003**, 103, 1917-1954.
19. Šimek, L.; Petřík, S.; Hadobaš, F.; Bohdanecký, M. *European Polymer Journal* **1990**, 26, (3), 375-377.
20. Lang, J. C.; Morgan, R. D. *Journal of Chemical Physics* **1980**, 73, (11), 5849-5861.